Design and Analysis of Drive System of Schatz Geometry Shaker Mixer

Sarpale S. A. 1, Prof. Swami M. C.2
[1] Student of M.S. Bidve Engineering College, Latur, Maharastra, India
[2] Professor Department of Mechanical Engineering, M.S. Bidve Engineering College, Latur, Maharastra, India

Abstract **- Mixing of two or more materials (i.e. heavy density metal powder in the fluid) is very difficult. In conventional method of mixing the metal powder and fluid mixing is carried out on unidirectional stirring machine. This paper investigates the limitations of the conventional mixer. The stirrer of conventional mixer rotates in one direction only which create a particular flow pattern in the fluid hence particles tend to stick to the wall of container due to centrifugal force. Most of the materials are settle down below the container due to high density. In conventional mixer, the other main issue is the vibrations, thrust and bending forces that create noise and high maintenance of machine. The research work is based on the Schatz geometry shaker mixer which is used for a homogeneous mixing of powdery substances with differing specific weights and particle sizes. The product is mixed in its own closed container. The mixing container is set into a three dimensional movement that use of rotation, translation and inversion according to the Schatz geometric theory. It is design, development, and analysis of driving system of Schatz mechanism with 3D-motion mixer to produce desired motion pattern, increase mixing rate and quality.**

Keywords- **conventional mixer, inversion, Schatz mechanism, Shaker Mixer.**

2. PROBLEM DEFINITION

Proposed Schatz geometry linkage with newly input system will gives homogeneous mixing of powdery substances with different specific weights and particle sizes. 3-dimensional Schatz geometry linkage will design, develop and analyze to produce desired motion pattern to achieve desired mixing rate and quality. Developed Schatz mechanism reduces cycle time of mixing, improve viscosity and spread ability of mixture. The Turbula shaker-mixer is used for the homogeneous mixing of powdery substances with differing specific weights and particle sizes. The product is mixed in its own closed container. It is also possible to mix wet and dry components or different wet components. The production process is hygienic and dust-free, making the Turbula easy to clean.

The exceptional efficiency of the Turbula shaker-mixer comes from the use of rotation, translation, and inversion according to the Schatz geometric theory.

The mixing container is set into three-dimensional movement that exposes the product to always changing, rhythmically pulsing motion. The results fulfill the highest requirements and are achieved in a minimum of time.

3. LITERATURE REVIEW

3.1 LITERATURE REVIEW OF DIFFERENT POWDER MIXING DEVICES.

Ingrid Bauman, Du Ska,Curi C and Matija Boban have discussed about mixing of solids in different mixing devices. Static mixers, as well as Turbula and V-shaped drum mixer were commonly used for powder blending in industry. Mixtures that were blended by means of those three devices were made out of the model material, quartz sand, in different component ratios (20:80 and 30:70). The results were statistically calculated and graphically presented. The results obtained by those three devices, the particle size effect and cohesion indexes, bring us to the conclusion that static mixers could be used for mixing of powders, but their shape, number of mixing elements and the mixer length should be adapted for each mixture separately, experimentally and mathematically, through modeling of the system.

3.2 LITERATURE REVIEW OF KINEMATIC ANALYSIS OF SCHATZ LINKAGE.

C-C Lee and J S Dai have investigates different configurations of the Schatz linkage which is based on the analysis of a reciprocal screw and relationship between the reciprocal screw and its stem-screw system, which consists of twists of freedom located at six revolute joints of the linkage. A new method of using cofactors of an augmenting screw is used to obtain the reciprocal screw. The stem-screw system of order 5 of the linkage is developed from the special geometry of the six revolute joints and closed-form displacement solutions are provided based on the stem-screw system. The screw surface representing the trajectory of the reciprocal screw with a chosen pitch is established. This surface is then used to characterize zero-pitch reciprocal screw configurations. The special relationship between the reciprocal screw and the stem-screw system is analyzed and used to characterize the constraint wrench and configurations created by the changes of the constraint wrench with a non-zero pitch. Consequently, a set of configurations are presented in conjunction with a ruled surface produced by the progression of the constraint wrench when the linkage drive joint rotates from 5˚ to 85˚. [9]

3.3 LITERATURE REVIEW OF SCHATZ MECHANISM AND ITS DRIVE SYSTEMS.

Donald I. Cruse have discussed about the apparatus which producing a combination of rotating, tumbling and shaking movements of material in a container has a closed and constrained invertible kinematic link-work of which at least one link serves

as receptacle for the container and motive power for driving the link-work is provided by imparting thrusting power, rather than rotating power. [17]

Reinhold C. invents the electric drive for the mixing machine. According to the invention, the drive for the inversion kinematic Paul Schatz type mixing machine consists of two electric motors (11, 12) in series powered at a constant current via a shared regulator. The current which determines the torque at the spindles (4, 5) is set by an adjuster. The voltage drop across the motors determines the mean revolution speed of shafts (4, 5) which rotate differentially owing to the design of the machine. The mixing machine, which is consist of a support (1) having two bearings (2, 3) in which the two parallel shafts (4, 5) can rotate. At their upper ends the shaft (4, 5) takes the form of swivel bearings (6) for two forks (7). Axis bolts for rotation (8) run through the forks (7) which are perpendicular to each other and to the respective swivel axes (6). The two axis bolts for rotation (8) are secured to a cage (9) receiving a mixing container (10). [18]

Richard S. Hartenberg, and Jacques Denavit gives the brief information about Schatz inversion linkage, also discuss about its velocity and acceleration diagrams and mechanisms behind that linkage. He discussed about the different driving systems of Schatz mechanism like electrical motors, pneumatic cylinders, and piston-cylinder. [19]

3.4 LITERATURE REVIEW OF QUALITY OF MIXTURE

Yong Kweon Suh and, Sangmo Kang have investigates mixing of micro fluids. They review the various designs of mixers that were used in different applications. They have classify the designs in terms of the driving forces, including mechanical, electrical and magnetic forces, used to control fluid flow upon mixing. The advantages and disadvantages of each design will also be addressed. Finally, they have given the expected future development regarding mixer design and related issues for the further enhancement of mixing performance.

Benjamin Ivorra, Juana L. Redondo, Juan G. Santiago, Pilar M. Ortigosa and Angel M. Ramos have performed the experiment on 2D and 3D modeling and optimization for the design of a fast hydrodynamic focusing micro fluidic mixer. They verify the robustness of the optimized result by performing a sensitivity analysis of its parameters. They achieve a design with a predicted mixing time of 0.10 μs, approximately one order of magnitude faster than previous mixers.

4. OBJECTIVES:

1. Estimation of the torque and power requirements of mixer for mixing of specified viscous fluids for given volume of mixture considering fluid friction in container, bearing friction in linkages etc.
2. Design and analysis of kinematic linkage to drive the Schatz geometry linkage.
3. Design development of locking mechanism of mixing container inside bracket such that container single degree of freedom i.e., rotation about own axis to add to effective mixing characteristics

5. METHODOLOGY:

- **Study literature review:**

Study various configurations of Schatz geometry linkage, also study different driving technologies for Schatz geometry linkage by using various technical papers, handbooks, patent documents etc.

- **Design and Development:**

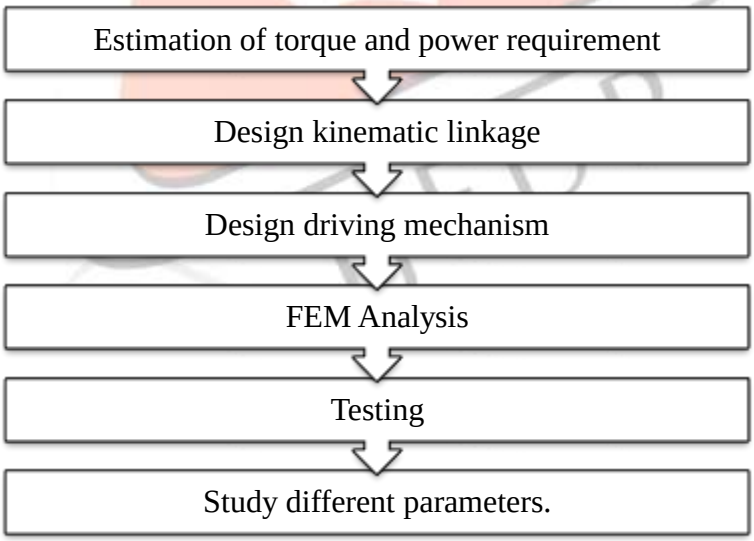

Fig. Methodology

1. Estimation of the torque and power requirements of mixer for mixing of specified viscous fluids for given volume of mixture considering fluid friction in container, bearing friction in linkages.
2. Design development of locking mechanism of mixing container inside bracket such that container single degree of freedom that is rotation about own axis to add to effective mixing characteristics by modeling the components using Unigraphix software, meshing using ANSYS to find equivalent stresses.
3. Selection of motor drive and worm gear box for driver linkage of the Schatz geometry 3d-motion mixer.

6. ESTIMATION OF THE TORQUE AND POWER REQUIREMENTS OF MIXER (THEORETICAL CALCULATIONS AND FE ANALYSIS)

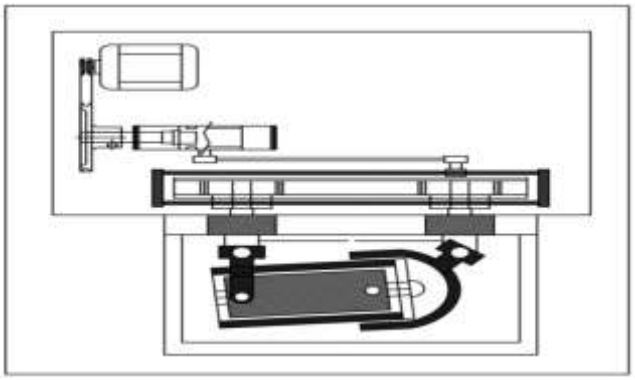

Fig. Line diagram of Schatz geometry 3D motion mixer.

Design of 3-d mixing machine
Input data (Ref. www.engineering toolbox.com)

1. Kinematic viscosity of Paint = 3.4 poise

$$= \frac{3.4}{0.01} \text{ centipoise}$$
$$= 340 \text{ Centipoise}$$

2. Specific gravity of paint = 1.89 kg/lit

In design of mixing machine the approach to design would be to calculate the torque required at the Input shaft for tumbling of the paint mixture to create the desired mixing action.

Total torque on Output shaft = Torque owing to viscous force + Torque owing static weight

Torque owing to viscous force inside container:

Here we have developed the container for unit volume i.e., 1 litre for which container size is 90 mm diameter and 160 mm length. .As the paint mixture is rotated along with the container for the third dimension action in the set up other than tumbling action caused by the Schatz geometry.

Given: $\mu = 3.4$ poise $= \frac{1}{10\times3.4} = 0.34$ Ns/m^2

Speed of tumbling = 30 rpm

Tangential speed of shaft = $u = \frac{\pi\times D\times N}{60}$

$$= \frac{\pi\times0.09\times30}{60}$$
$$= 0.142\text{m/sec}$$

Now,

$\tau = \mu \, du/dy$

Where;

τ = Shear stress (N/m^2)

Considering the paint remains stagnant at the centre of container

du = Change in speed = u-0 = 0.142 m/sec

dy = Distance between wall and the centre = 0.045m

$$\tau = \frac{0.34 \times 0.142}{0.045}$$
$$= 1.072 \text{ N/m}^2$$

Area of the cylinder that is exposed to this shear intensity will be the circumferential area

$A = \pi \times D \times w = \pi \times 0.09 \times 0.16 = 0.045\text{m}^2$

Shear force (F) = Shear stress x Shear area

$= 1.072 \times 0.045$

$= 0.048\text{N}$

Power = F x u =0.048 x 0.142 =6.816 x10^{-3} watt / stroke

Thus total power required = 6.816 x10^{-3} x 30 x2 = 0.408 watt

Calculation of Torque owing to weight of container

Weight of container system is derived as follows:

Weight of container system = Weight of empty container + weight of paint - weight of Link mechanism

Considering container dimensions to be 96 mm outside diameter and 160 mm length and 3 mm overall thickness.

Weight of empty container = 0.56 kg

Weight of paint = 1.89 kg

Weight of linkage = 0.4 kg max.

Force required to lift container = weight of container system x 9.81 = 2.85 x 27.95 N

Toque required to tumble container = T = µRn x R

Coefficient of friction (µ) = 0.5

Table: Material Details

Coefficient of friction for a range of material combinations				
Combination	**Static**		**Dynamic**	
	dry	**Lubricated**	**Dry**	**lubricated**
steel-steel	0.5...0.6	0.15	0.4...0.6	0.15

R = radius of turning of the linkage = opening of the linkage/2

R= 190 /2 = 95 mm

T= 0.5 x 27.95 x 95 = 1327 N-mm

Thus power required for tumbling action = $\frac{\pi \times 2 \times 30 \times 1.327}{60}$

=4.2 watt

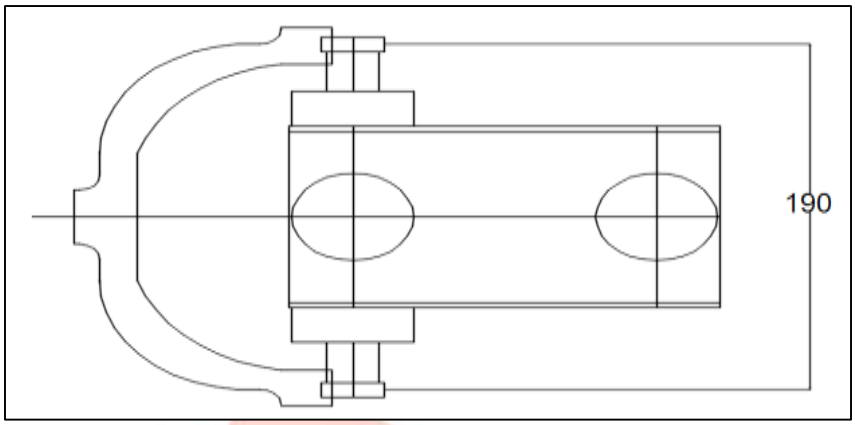

Fig. Schatz Linkage Bracket

Total torque on Output shaft = Torque owing to viscous force + Torque owing static weight

= 4.2 + 0.48 = 4.68.

Thus total power required = 5 watt approx.

Now the Schatz geometry linkage is a 3-d linkage with considerable amount of friction in the universal joint elements more over the transmission the driver linkage comprises of rack- pinion , self-locking worm gear drive (efficiency less than 50%) as it is required that linkage should not turn back under action of container weight and thus provide self-locking.

Thus it is safe to assume 30% power transmission efficiency of the drive, thus the net power required will be 5 + 0.7 (5) = 8.5 watt …thus selecting following motor:

A. Motor Selection

The selecting a motor of the following specifications

Single phase AC motor

Commutator motor

TEFC construction

Power = 50 watt

Speed= 0-9500 rpm (variable)

B. Design of Belt Drive

Power is transmitted from the motor shaft to the input shaft of drive by means of an open belt drive,

Motor pulley diameter = 20 mm

IP _ shaft pulley diameter = 100 mm

Reduction ratio = 5

IP shaft speed = 9500/5 = 1900 rpm

T motor = 0.05 N-m

Torque at IP shaft = 5 x 0.05 = 0.25 Nm

Design of Open Belt Drive

Motor pulley diameter = 20 mm

IP shaft pulley diameter = 110 mm

Reduction ratio = 5

Coefficient of friction = 0.23

Maximum allowable stress in belt = 7 Mpa

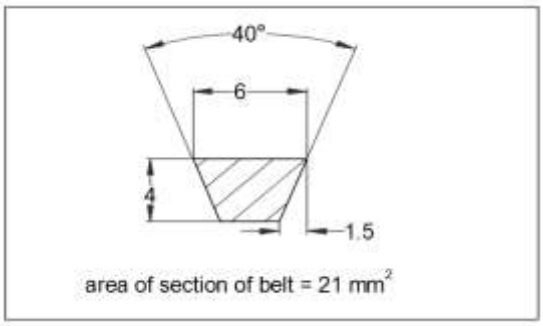

Fig. Section of V-belt

Area of belt =21 mm^2
Maximum allowable tension in belt = Maximum allowable stress x area
= 7 x21 =147 N

Center distance = 200
$\alpha = 180 - \sin^{-1} (D-d)/2C$
$\alpha = 180 - \sin^{-1} (110-20)/2x200$
$\alpha = 136^0$
$\alpha = 2.37^c$
Now,
$e^{\mu\alpha/\sin(\theta/2)} = e^{0.2 \times 2.37 \sin(40/2)} = 4$
Width (b_2) at base is given by
$b_2 = 6-2(4 \tan 20) = 3.1$
Now mass of belt /m length = 0.23 kg/m
$V = \pi DN/ (60 \times 1000) = 4.188$m/sec
$Tc = m V^2$
Tc = 4.034 N
T_1 = Maximum tension in belt – Tc
T_1= 147 – 4.034 = 142.9 N
$T_1 / T_2 = e^{\mu\alpha/\sin(\theta/2)} = 4$
T_2 = 35.74 N

Power transmitting capacity = (T_1-T_2) v = (142.9-35.4)x4.81/1000 = 21.5 Kw
Thus the belt can safely transmit power of 0.05 Kw

$$fdesign = \frac{P \times 60}{2 \times \pi \times 9500}$$
= 0.252 N-m

Reduction ratio of pulley drive = 100 /20 = 5

C. Design of Worm and Worm Wheel

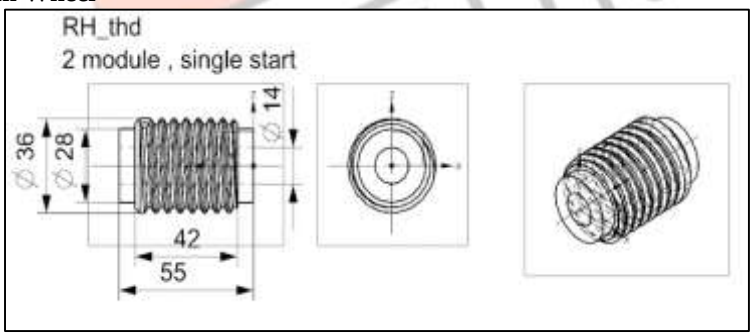

Fig. Geometry of Worm

Table: Design data of Worm

Designation	Ultimate Tensile Strength N/mm²	Yield Strength N/mm²
20MnCr1	1000	800

$$fs_{allowable} = 0.18 \times 1000 = 180 N/mm^2$$
$$Tdesign = 0.252 Nm$$

Check for Torsional Shear Failure of Shaft.

$$Td = \frac{\pi fs_{act} \times}{16 \times D} D^4 - d^4$$
$$fs_{act} = \frac{16 \times Td \times D}{\pi \times D^4 - d^4}$$

$$fs_{act} = \frac{16 \times 2 \times 10^3 \times 36.4}{\pi \times 36.4^4 - 21^4}$$

fs_{act} = 0.23 N/mm^2

As $fs_{act} < fs_{all}$

Worm is safe under torsional load.

ANALYSIS OF WORM

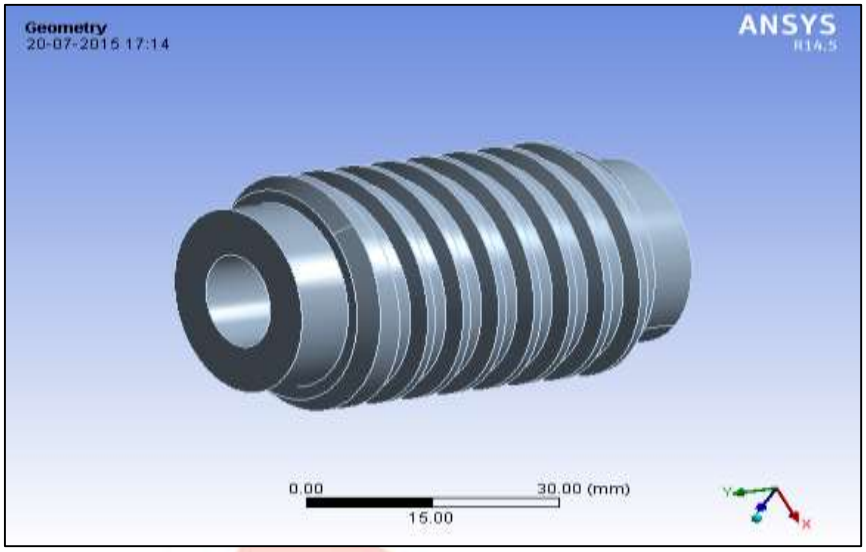

Fig. 3.7 Geometry of worm

This is the geometry of worm drawn in Solid Works. This worm used to transmit the power from worm shaft to worm wheel. 20MnCr1 material is used for manufacturing the shaft having ultimate strength is 1000 N/mm^2 and yield strength is 800 N/mm ^{2}. The model of worm prepared using Solid Works software and it is imported into the ANSYS. After importing the model material properties like modulus of elasticity (N/mm ^{2}), Poisson's ratio and density (Kg/mm ^{3}) etc. was defined.

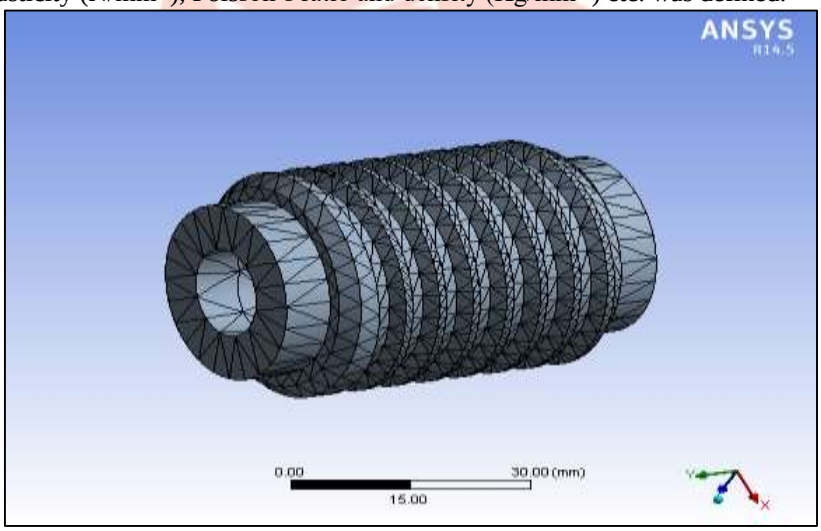

Fig. 3.8 Meshing of Worm

Above worm geometry used for meshing.

No of Elements	3643
No of Nodes	2046
Type of element	Tetrahedral
Type of Meshing	Solid mesh

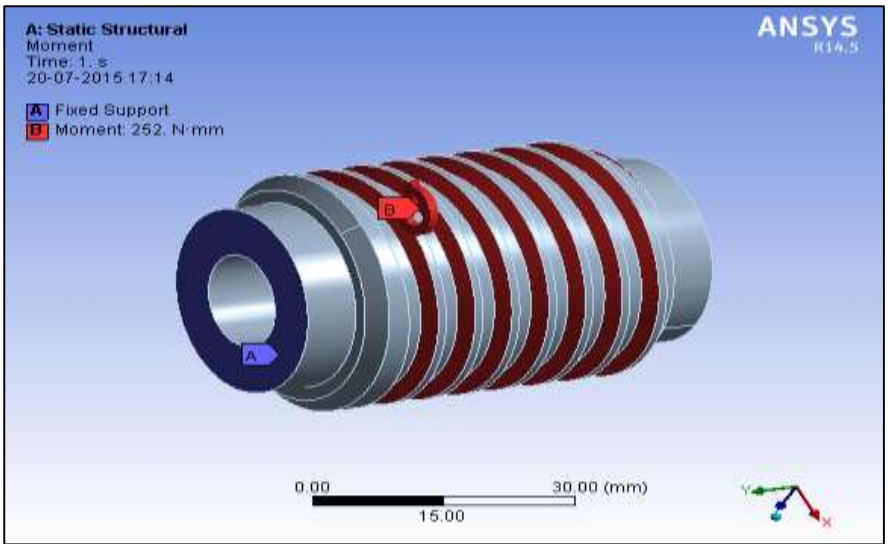

Fig.3.9 Boundary conditions to the Worm

A worm having anticlockwise moment will be act in the y-axis direction which magnitude is 252 N.mm. Its moment components are (0, 252, 0).

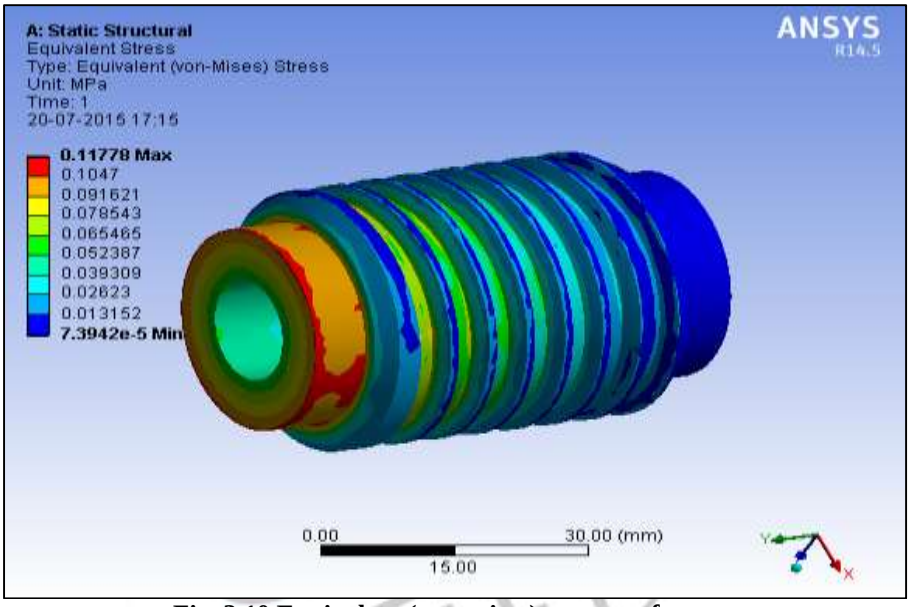

Fig. 3.10 Equivalent (von-mises) stresses of worm

Fig. 3.10 shows the maximum equivalent (Von-Mises) stress of the worm is 0.11778 N/mm^2 and the stress by analytical method is 0.23 N/mm^2.

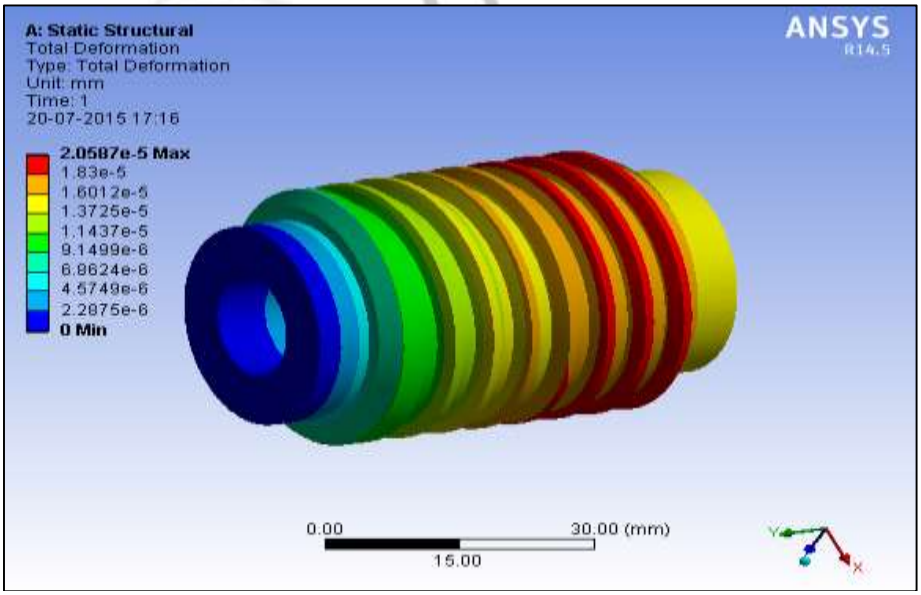

Fig. 3.11 Total deformation of worm

Worm gear shows 2.0587e-5 i.e. negligible deformation under the action of system of forces.

Result & discussion

Table No.3.3 Result & discussion of worm

Part Name	Maximum theoretical stress (MPa)	Von-mises stress (MPa)	Maximum deformation (mm)	Result
WORM	0.23	0.1178	2.05E-5	safe

1. Maximum stress by theoretical method and Von-Mises stress are well below the allowable limit, hence the worm is safe.
2. Worm shows negligible deformation under the action of system of forces.

C) Design of Worm Wheel:

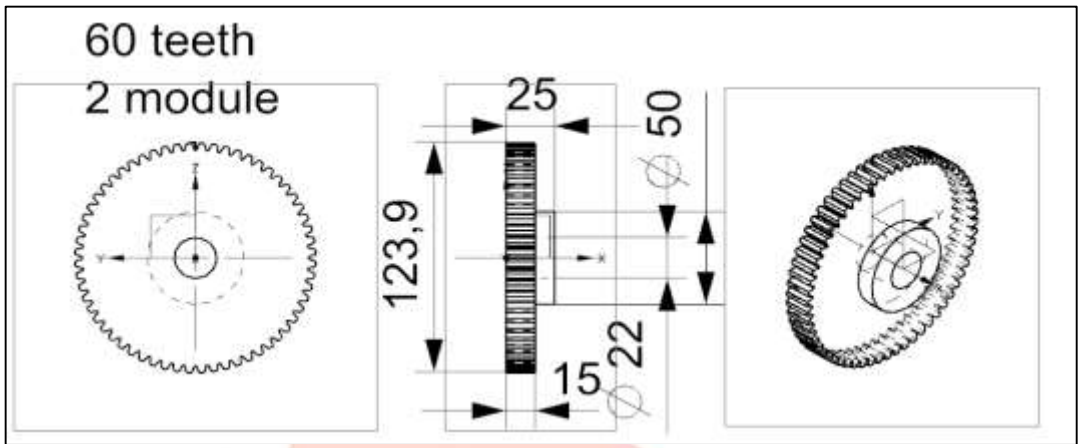

Fig. 3.12 2-D Geometry of worm wheel

Table No.3.4 Design data of worm wheel

Designation	Ultimate Tensile Strength N/mm^2	Yield Strength N/mm^2
20MnCr1	1000	800

$$fs_{allowable} = 0.18 \times 1000 = 180 N/mm^2$$
$$Tdesign = 0.252 \times 60 = 15.12 Nm$$

Check for Torsional Shear Failure of Shaft.

$Td = \frac{\pi f s_{act} \times}{16 \times D}$ D^4- d^4

$$fs_{act} = \frac{16 \times Td \times D}{\pi \times D^4 - d^2}$$
$$fs_{act} = \frac{16 \times 15.12 \times 10^3 \times 50}{\pi \times 50^4 - 22^4}$$
fs_{act} = 0.639 N/mm^2

As $fs_{act} < fs_{all}$

Worm gear is safe under torsional load.

The pair of worm and worm wheel used in the machine is designated as

1/60/10/2

The worm is made of case hardened steel 14C6 and the worm wheel is made of Cast iron.

No. of starts on Worm = Z_1 = 1

No. of Teeth on Worm Wheel = Z_2 = 60

Diametral Quotient = q= 10

Module = m = 2 mm.

Speed Ratio = i = $\frac{Z_2}{Z_1}$ = 60 mm.

Worm Input Shaft Speed = N_1 = 1900 rpm

Worm Wheel Output Shaft Speed = N_2 = 1900/60 = 31.66=30 rpm appro.

Tangential tooth load = Wt = T/r = 15120 /60 =252 N

Now strength of worm gear is given by,

Wt = σ Cv b π m y

Where,

σ = 84 Mpa

b= 15mm

m= module =2mm
y = form factor = 0.124 -(0.684 /Tg) = 0.1126
Cv = 6 /(6 +v) = 6 /(6 + 3.142) = 0.656 ----(v = 2πN/60)
σmax = 252 / 0.656 x 15 x 2 x 3.142 x 0.1126 = 36.19
As, σ act < σ allowable
Thus the gear is safe.

ANALYSIS OF WORM GEAR

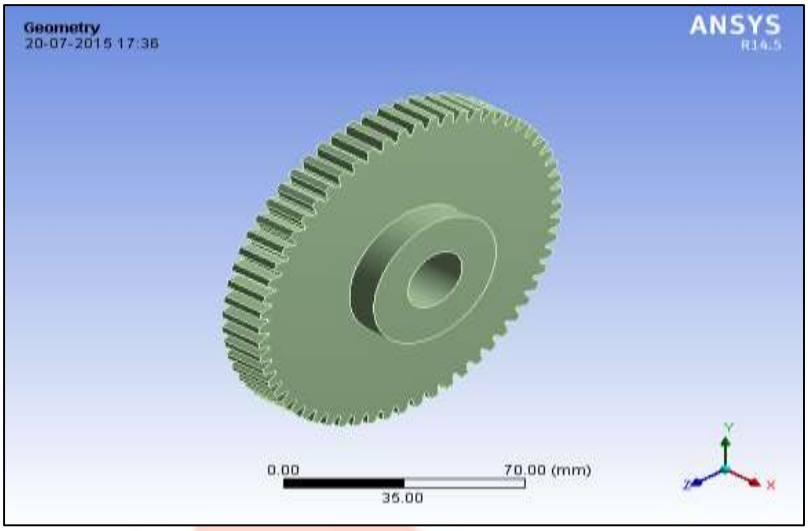

Fig. 3.13 Geometry of worm wheel

This is the geometry of worm wheel drawn in Solid Works. This worm wheel used to transmit the power from worm to worm wheel shaft. 20MnCr1 material is used for manufacturing the shaft having ultimate strength is 1000 N/mm^2 and yield strength is 800 N/mm ^{2}.

The model of worm wheel shaft prepared using Solid Works software and it is imported into the ANSYS. After importing the model material properties like modulus of elasticity (N/mm ^{2}), Poisson's ratio and density (Kg/mm ^{3}) etc. was defined. Then proper element type was selected (having required number of degrees of freedom). For particular material real constant set was defined. To obtain the accurate results fine meshing of the above plate model have been done.

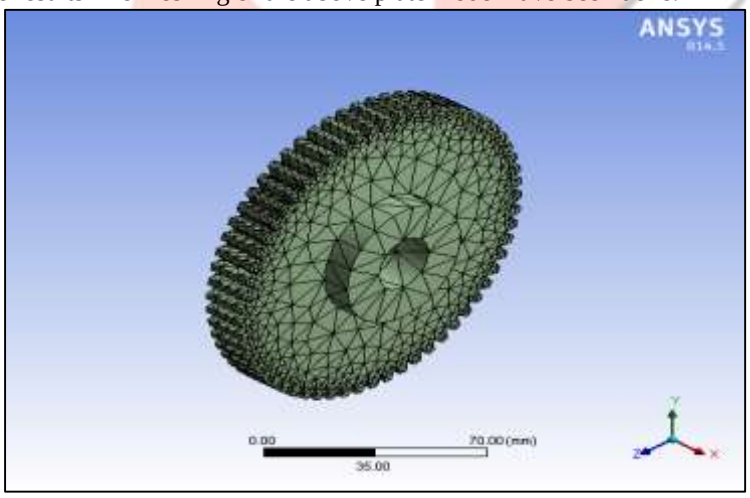

Fig. 3.14 meshing of worm wheel

Above worm wheel shaft geometry used for meshing.

No of Elements	3643
No of Nodes	2046
Type of element	Tetrahedral
Type of Meshing	Solid mesh

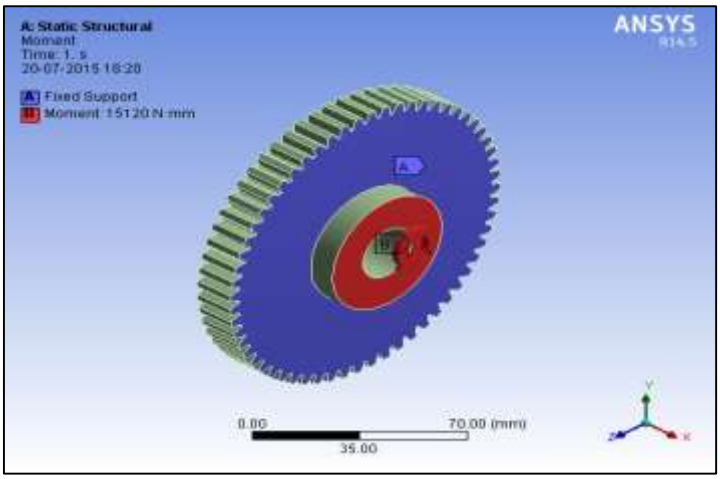

Fig.3.15 Boundary conditions to the Worm wheel

A worm wheel having clockwise moment will be act in the y-axis direction which magnitude is 15120 N.mm. Its moment components are (0, 15120, 0).

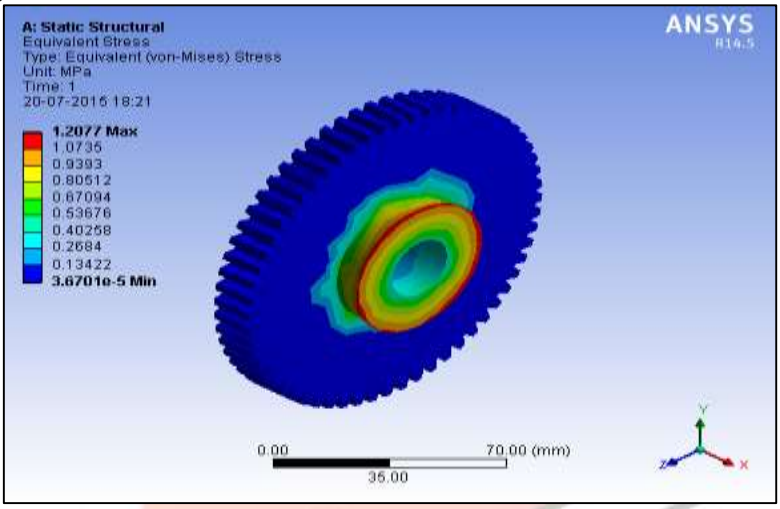

Fig. 3.16 Equivalent (Von-Mises) stresses of worm wheel

Fig. 3.16 shows the maximum equivalent (Von-Mises) stress of the worm wheel is 1.207 N/mm^2 and the stress by analytical method is 0.639 N/mm^2.

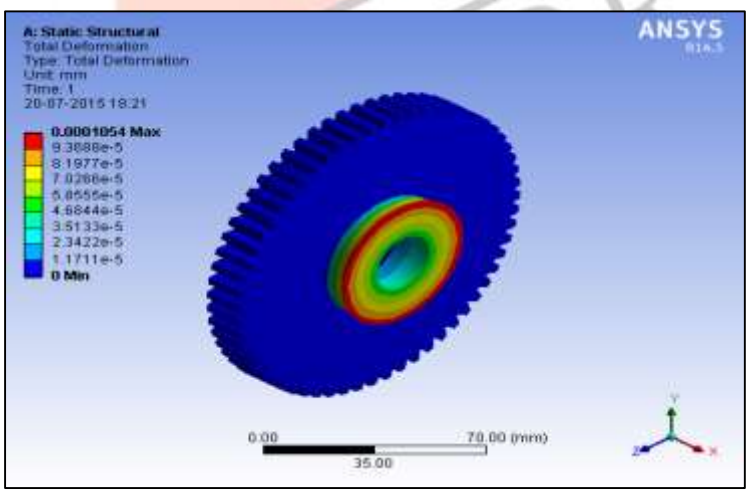

Fig. 3.17 Total deformation of worm wheel

Worm gear shows 1.054e-5 i.e. negligible deformation under the action of system of forces.

Result & discussion

Table No.3.5 Result & discussion of worm wheel

Part Name	Maximum theoretical stress (MPa)	Von-Mises stress (MPa)	Maximum deformation (mm)	Result
Worm Gear	0.639	1.027	0.0001054	safe

1. Maximum stress by theoretical method and Von-Mises stress are well below the allowable limit hence the worm gear is safe.
2. Worm gear shows negligible deformation under the action of system of forces.

D. Design of Worm Shaft:

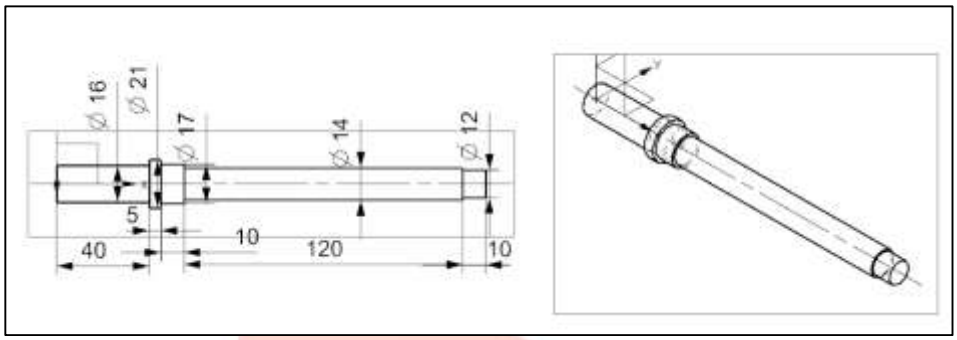

Fig. 3.18 2-D Geometry of worm shaft

Material Selection:

Table No.3.6 Design data of worm shaft

Designation	Ultimate Tensile Strength (N/mm^2)	Yield Strength (N/mm^2)
EN 24	800	680

ASME Code for Design of Shaft

The loads on the shafts in connected machinery are not constant, it is necessary to make proper allowance for the harmful effects of load fluctuations. According to ASME code permissible values of shear stress may be calculated from various relations.

= 800/2 = 400 N/mm^2

$$fs_{max} = \frac{fut}{\text{FOS}}$$

$$fs_{max} = \frac{800}{2}$$

$$fs_{max} = 400\ N/mm^2$$

This is the allowable value of shear stress that can be induced in the shaft material for safe operation.

Check for torsional shear failure of shaftN/mm^2

$$Te = \frac{\pi \times fs_{act} \times d^3}{16}$$

$$fs_{act} = \frac{16 \times 0.252 \times 10^3}{16}$$

$$fs_{act} = 0.742\ N/mm^2$$

As; $fs_{act} < fs_{all}$

Worm shaft is safe under torsional load.

ANALYSIS OF WORM SHAFT

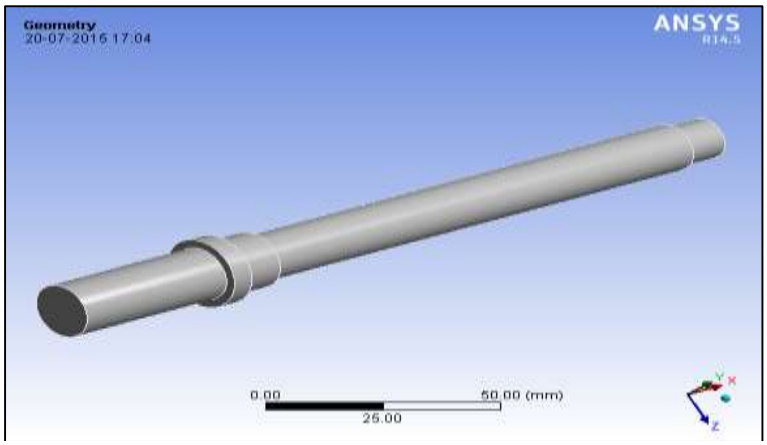

Fig. 3.19 Geometry of worm shaft

This is the geometry of worm shaft drawn in Solid Works. This worm shaft used to transmit the power from pulley to worm. EN 24 materials is used for manufacturing the shaft having ultimate strength is 800 N/mm^2 and yield strength is 680 N/mm ^{2}.

The model of worm shaft prepared using Solid Works software and it is imported into the ANSYS. After importing the model material properties like modulus of elasticity (N/mm ^{2}), Poisson's ratio and density (Kg/mm ^{3}) etc. was defined. Then proper element type was selected (having required number of degrees of freedom). For particular material real constant set was defined. To obtain the accurate results fine meshing of the above plate model have been done.

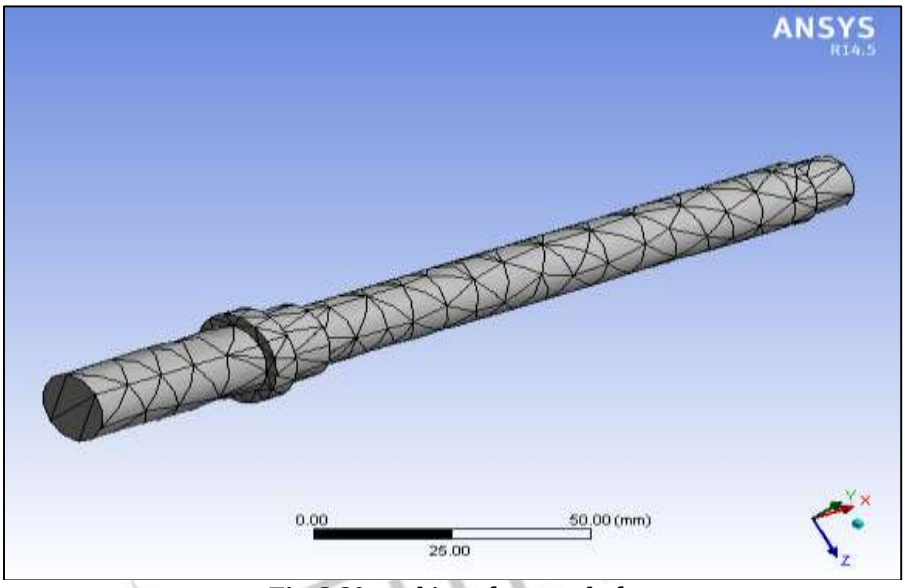

Fig. 3.20 meshing of worm shaft

Above worm shaft geometry used for meshing.

No of Elements	3643
No of Nodes	2046
Type of element	Tetrahedral
Type of Meshing	Solid mesh

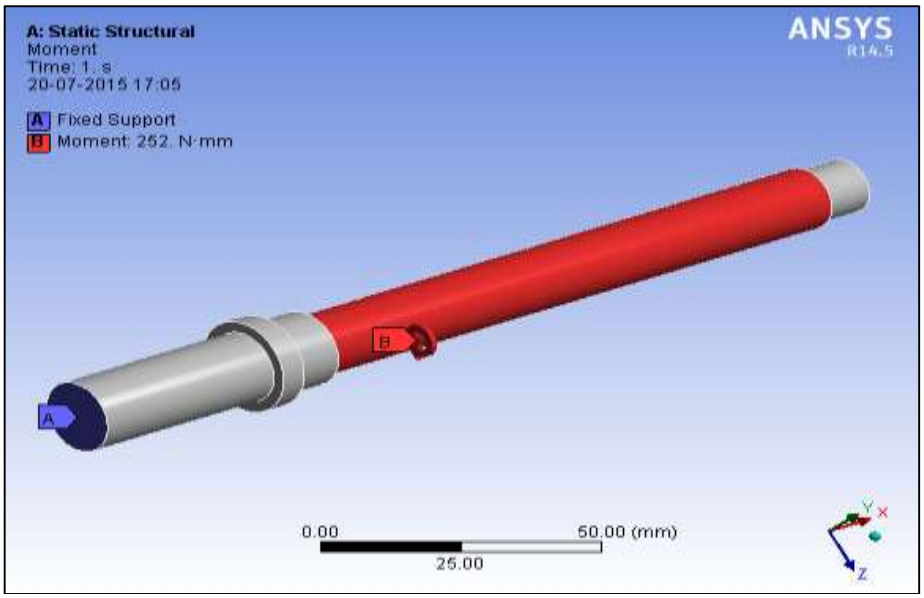

Fig.3.21 Boundary conditions to the Worm shaft

A worm shaft having clockwise moment will be act in the y-axis direction which magnitude is 252 N.mm. Its moment components are (0, 252, 0).

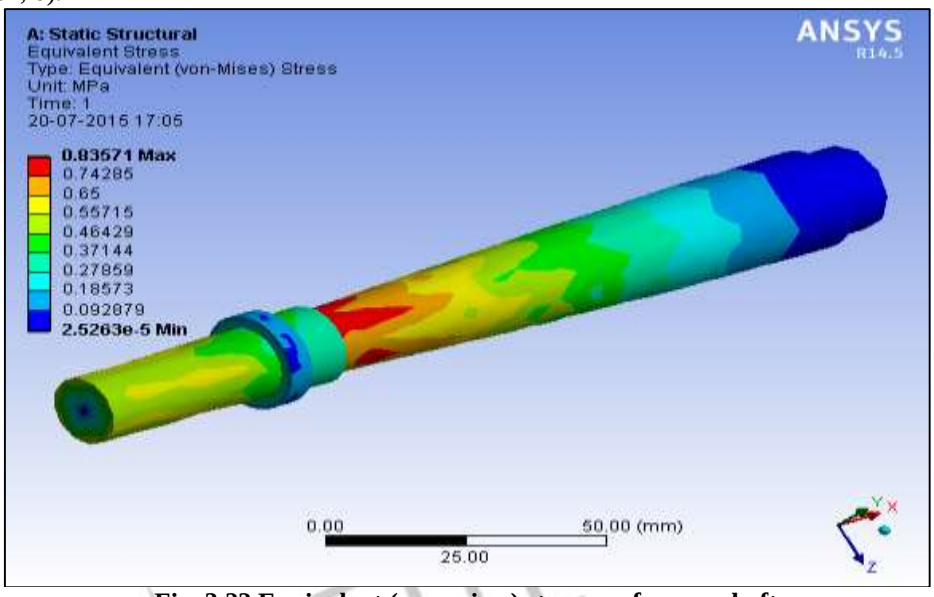

Fig. 3.22 Equivalent (von-mises) stresses of worm shaft

Fig. 3.22 shows the maximum equivalent (Von-Mises) stress of the worm wheel is 0.83571 N/mm^2 and the stress by analytical method is 0.742 N/mm^2.

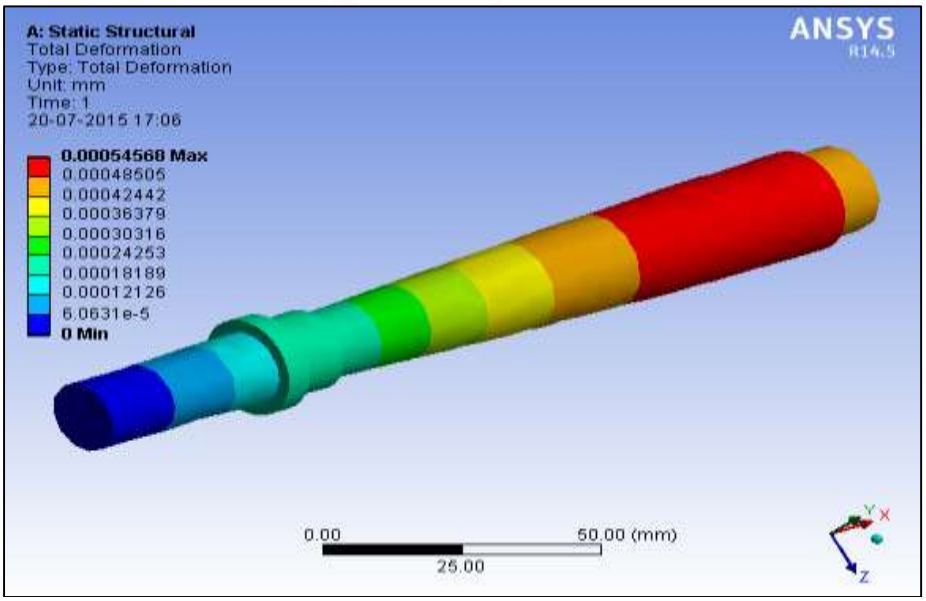

Fig. 3.23 Total deformation of worm shaft

Worm gear shows 4.05e-5 i.e. negligible deformation under the action of system of forces.

Result & discussion

Table No.3.7 Result & discussion of worm shaft

Part Name	Maximum theoretical stress (MPa)	Von-Mises stress (MPa)	Maximum deformation (mm)	Result
Worm Shaft	0.742	0.8357	0.00054	safe

1. Maximum stress by theoretical method and Von-Mises stress are well below the allowable limit hence the worm shaft is safe.
2. Worm shaft shows negligible deformation under the action of system of forces.

E. Design of Worm Wheel Shaft

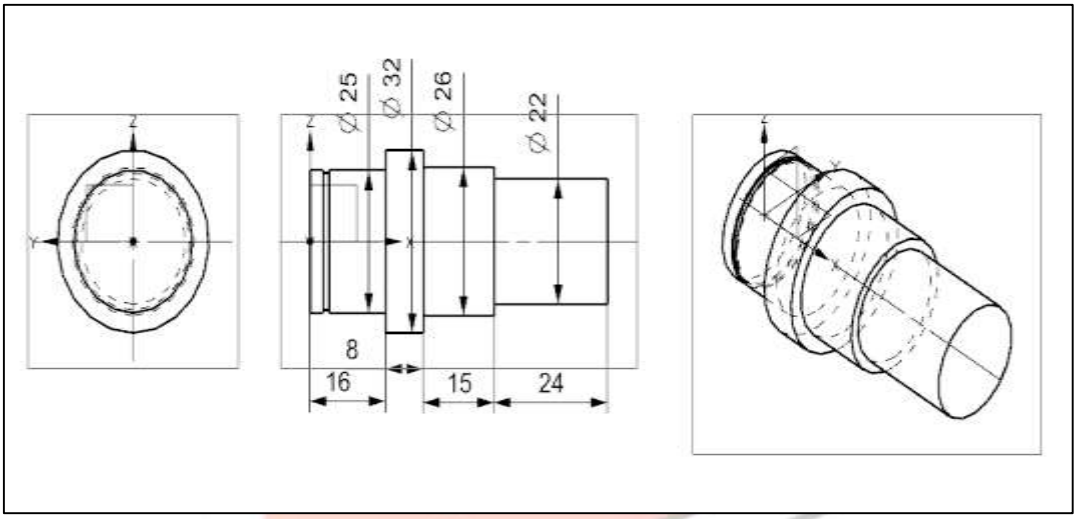

Fig. 3.24 2-D Geometry of worm wheel shaft

Table No.3.8 Design data of worm wheel shaft

Designation	Ultimate Tensile Strength N/mm²	Yield Strength N/mm²
EN24	800	680

$$fs_{allowable} = 0.18 \times 800 = 144 N/mm^2$$

T design = 15.12 Nm

This is the allowable value of shear stress that can be induced in the shaft material for safe operation.

Check for torsional shear failure of shaft

$$Te = \frac{\pi \times fs_{act} \times d^3}{16}$$

$$fs_{act} = \frac{16 \times 15.12 \times 10^3}{\pi \times 22^3}$$

$$fs_{act} = 7.23\ N/mm^2$$

As; $fs_{act} < fs_{all}$

Worm wheel shaft is safe under torsional load.

ANALYSIS OF WORM WHEEL SHAFT

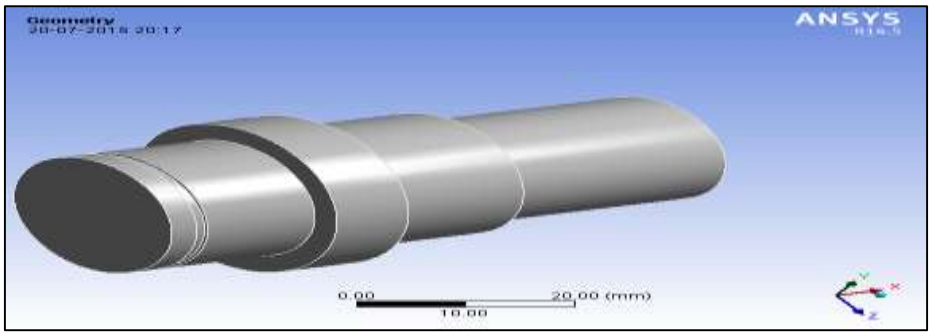

Fig. 3.25 Geometry of worm wheel shaft

This is the geometry of worm wheel shaft drawn in Solid Works. This worm wheel shaft used to transmit the power from worm wheel to reciprocating linkage. EN24 material is used for manufacturing the shaft having ultimate strength is 800 N/mm^2 and yield strength is 680 N/mm ^{2}.

The model of worm wheel shaft prepared using Solid Works software and it is imported into the ANSYS. After importing the model material properties like modulus of elasticity (N/mm ^{2}), Poisson's ratio and density (Kg/mm ^{3}) etc. was defined. Then proper element type was selected (having required number of degrees of freedom). For particular material real constant set was defined. To obtain the accurate results fine meshing of the above plate model have been done.

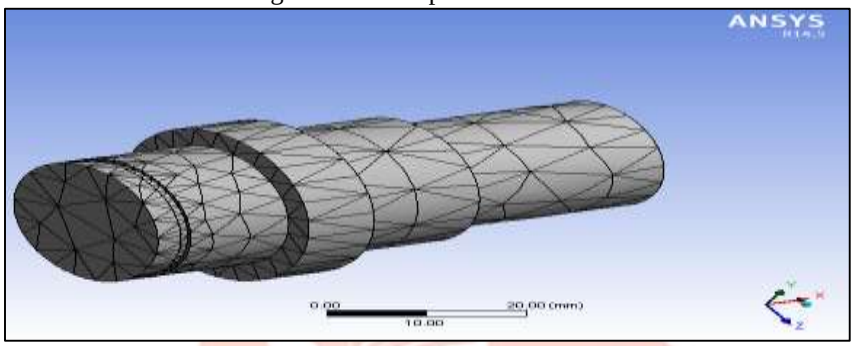

Fig. 3.26 meshing of worm wheel shaft

Above worm wheel shaft geometry used for meshing.

No of Elements	3643
No of Nodes	2046
Type of element	Tetrahedral
Type of Meshing	Solid mesh

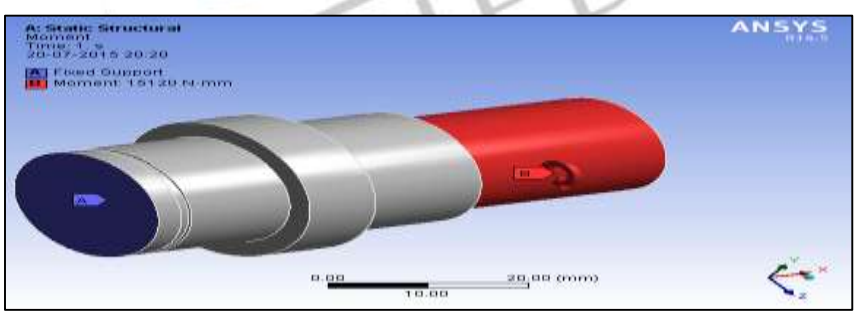

Fig.3.27 Boundary conditions to the Worm wheel shaft

A worm wheel shaft having clockwise moment will be act in the y-axis direction which magnitude is 15120 N.mm. Its moment components are (0, 15120, 0).

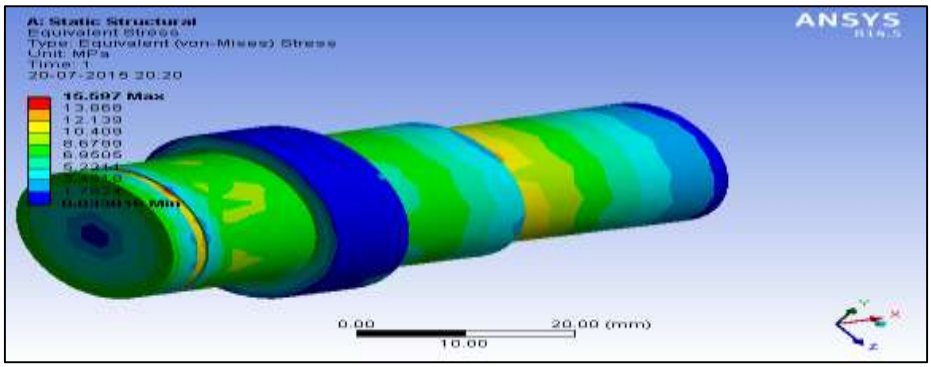

Fig. 3.28 Equivalent (von-mises) stresses of worm wheel shaft

Fig. 3.16 shows the maximum equivalent (Von-Mises) stress of the worm wheel is 15.597 N/mm^2 and the stress by analytical method is 7.23 N/mm^2.

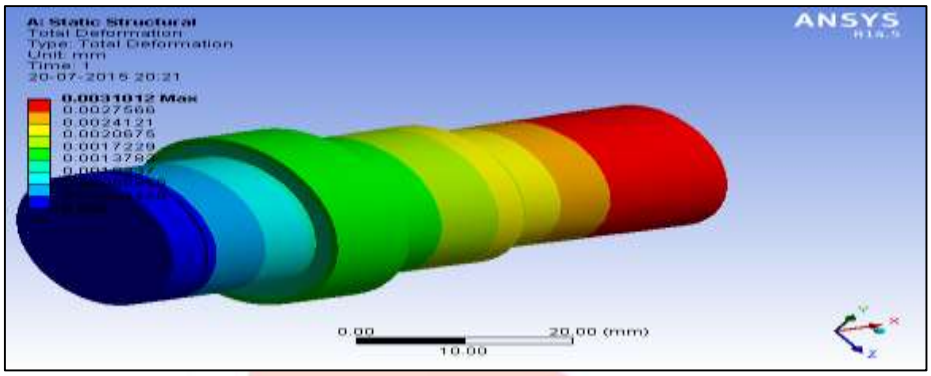

Fig. 3.29 Total deformation of worm wheel shaft

Worm gear shows 3.10e-5 i.e. negligible deformation under the action of system of forces.

Result & discussion

Table No.3.9 Result & discussion of worm wheel shaft

Part Name	Maximum theoretical stress (MPa)	Von-mises stress (MPa)	Maximum deformation (mm)	Result
Worm Gear Shaft	7.23	15.597	0.00312	safe

1. Maximum stress by theoretical method and Von-Mises stress are well below the allowable limit hence the worm gear shaft is safe.
2. Worm gear shafts show negligible deformation under the action of system of forces.

F. Design of Input Shaft Ball Bearing:

In selection of ball bearing the main governing factor is the system design of the drive i.e., the size of the ball bearing is of major importance, hence we shall first select an appropriate ball bearing.

Ball Bearing Selection:

Series 62

Table No.3.10 Bearing selection for Input Shaft of worm

ISI NO	Brg. Basic Design No (SKF)	D	D1	D	D2	B	Basic capacity	
							C kgf	Co Kgf
17A C02	6003	17	19	35	33	10	465	285

Equivalent dynamic load,

$$P = XF_r + YF_a$$

Where,

P=Equivalent dynamic load, (N)
X=Radial load constant
Fr= Radial load (N)
Y = Axial load contact
F_a = Axial load (N)
In our case,
Radial load F_R= 750N
Axial load F_a= Maximum table load = 60 kg =600 N

$$P = 0.56 \times 750 + 1.8 \times 600$$
$$P = 1500N$$

Considering 4000 working hours

$$L_h = \frac{16667}{n}\left(\frac{c}{p}\right)^3$$
$$4000 = \frac{16667}{20}\left(\frac{c}{1500}\right)^3$$
$$C = 2530.28\ N$$
$$C = 258.19\ Kgf$$

Required dynamic load of bearing is less than the rated dynamic capacity of bearing, therefore bearing is safe.

G. Design of Worm Wheel Shaft Ball Bearing:

In selection of ball bearing the main governing factor is the system design of the drive i.e., the size of the ball bearing is of major importance, hence we shall first select an appropriate ball bearing.

Ball Bearing Selection:
Series 60

Table No.3.11Bearing selection for worm wheel Shaft

ISI NO	Brg. Basic Design No (SKF)	D	D1	D	D2	B	Basic capacity	
							C kgf	Co Kgf
20AC02	6004	20	23	42	36	12	735	450

Equivalent dynamic load,

$$P = XF_r + YF_a$$

Where,
P=Equivalent dynamic load, (N)
X=Radial load constant
Fr= Radial load (N)
Y = Axial load contact
F_a = Axial load (N)
In our case,
Radial load F_R= 750N
Axial load F_a= Maximum table load = 60 kg =600 N

$$P = 0.56 \times 750 + 1.8 \times 600$$
$$P = 1500N$$

Considering 4000 working hours

$$L_h = \frac{16667}{n}\left(\frac{c}{p}\right)^3$$
$$4000 = \frac{16667}{20}\left(\frac{c}{1500}\right)^3$$
$$C = 2530.28\ N$$
$$C = 258.19\ Kgf$$

Required dynamic load of bearing is less than the rated dynamic capacity of bearing, therefore bearing is safe.

H. Design of Input Shaft Ball Bearing:

In selection of ball bearing the main governing factor is the system design of the drive i.e., the size of the ball bearing is of major importance, hence we shall first select an appropriate ball bearing.

Equivalent dynamic load,

$$P = XF_r + YF_a$$

Where,
P=Equivalent dynamic load, (N)
X=Radial load constant

Fr= Radial load (N)
Y = Axial load contact

Ball Bearing Selection:

Series 60

Table No.3.12 Bearing selection for Input Shaft of worm wheel

ISI NO	Brg. Basic Design No (SKF)	D	D1	D	D2	B	Basic capacity	
							C kgf	Co Kgf
25A C02	6005	25	28	47	44	12	780	520

F_a = Axial load (N)

In our case,

Radial load F_R= 750N

Axial load F_a= Maximum table load = 60 kg =600 N

$$P = 0.56 \times 750 + 1.8 \times 600$$

$$P = 1500N$$

Considering 4000 working hours

$$L_h = \frac{16667}{n}\left(\frac{c}{p}\right)^3$$

$$4000 = \frac{16667}{20}\left(\frac{c}{1500}\right)^3$$

$$C = 2530.28\ N$$

$$C = 258.19\ Kgf$$

Required dynamic load of bearing is less than the rated dynamic capacity of bearing, therefore bearing is safe.

I. Design of Crank of Slider Crank Mechanism:

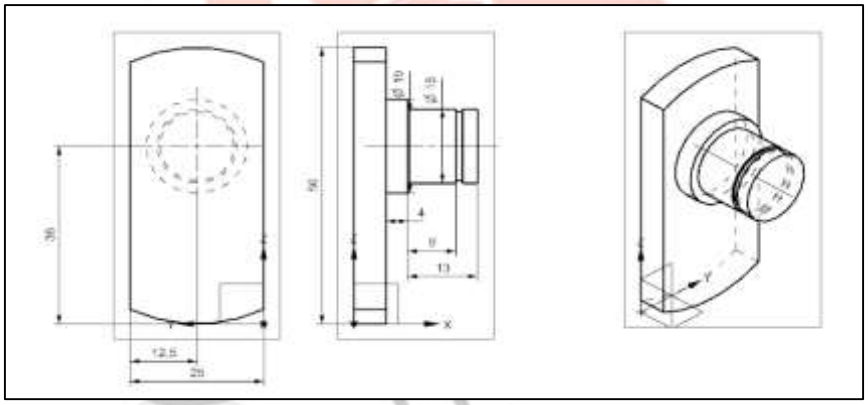

Fig. 3.30 2-D Geometry of crank

Table No. 3.13. Design data of Worm Crank

Designation	**Tensile Strength N/mm²**	**Yield Strength N/mm²**
EN9	600	480

Here radial load is due to the tangential load generated when the crank drives the connecting rod linkage at eccentricity of 25 mm

Load = Torque / radius = 15120 /25 =604 N

$$fs_{act} = \frac{W}{A}$$

$$fs_{act} = \frac{604 \times 4}{\pi \times 15^3}$$

$$fs_{act} = 3.41\ N/mm^2$$

As $fs_{act} < fs_{all}$

Crank is safe under shear load

J. Design of Connecting Rod

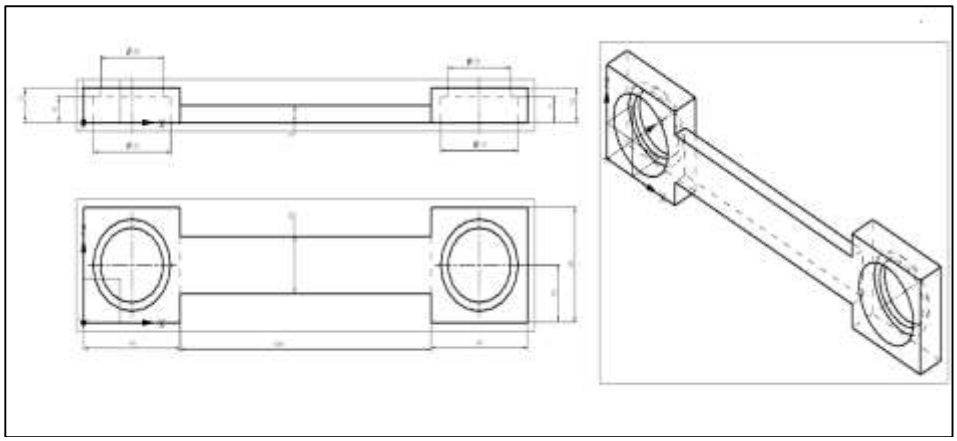

Fig. 3.36 2-D Geometry of Connecting Rod

Table No. 3.15. Design data of Connecting rod

Designation	**Tensile Strength N/mm²**	**Yield Strength N/mm²**
EN9	600	480

Direct tensile stress due to a pull load:-
Here Pull load is due to the tangential load generated when the crank drives the connecting rod linkage at eccentricity of 25 mm
Load = Torque / radius = 15120 /25 =604 N

$$fs_{act} = \frac{W}{A}$$

$$fs_{act} = \frac{604}{6 \times 20}$$

$$fs_{act} = 5.033\ N/mm^2$$

As $fs_{act} < fs_{all}$
Connecting rod is safe under shear load.

K. Design of Rack and Pinion

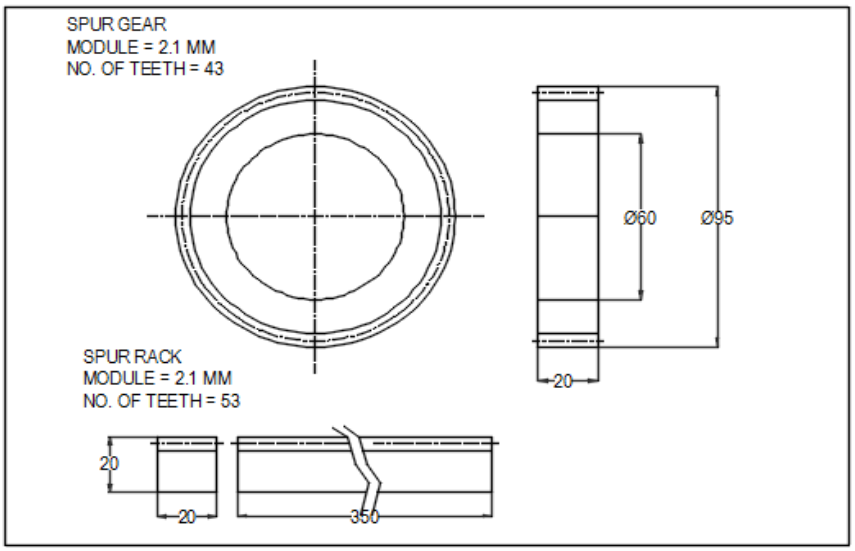

Fig. 3.42 2-D Geometry of Rack and Pinion

Input Data:
Load = 604 N
Material of pinion and gear is High steel EN24
Tensile strength =800 N/mm²
S_{ult} pinion = S_{ult} rack = 800 N/mm²
Considering Factor of Safety =3 As Rack Pinions Critical Part of Transmission
S_{ult} pinion = 800/3 =266.7
Service factor (Cs) = 1.5

d_p = 90.3

Lewis Strength equation

$$W_T = Sbym \quad (A)$$

Where;

Y= 0.484 – 2.86/Z

= 0.417

S_{yp} = 111.2

$W_T = (S_{yp})$ x b x m

=111.2 x 20x m

W_T= 2224m (B)

Equation (A) & (B)

2224m = 604

m=0.217

selecting standard module =2.1 mm, this is considering that for mechanism to work properly full depth of tooth engagement will be necessary with 2.1 module proper root clearance can b maintained along with full depth engagement of rack and pinion.

Gear Data

No. of teeth on pinion=43

No. of teeth on rack=53

Module = 2.1 mm

L. Design of Schatz Geometry Linkage Shaft:

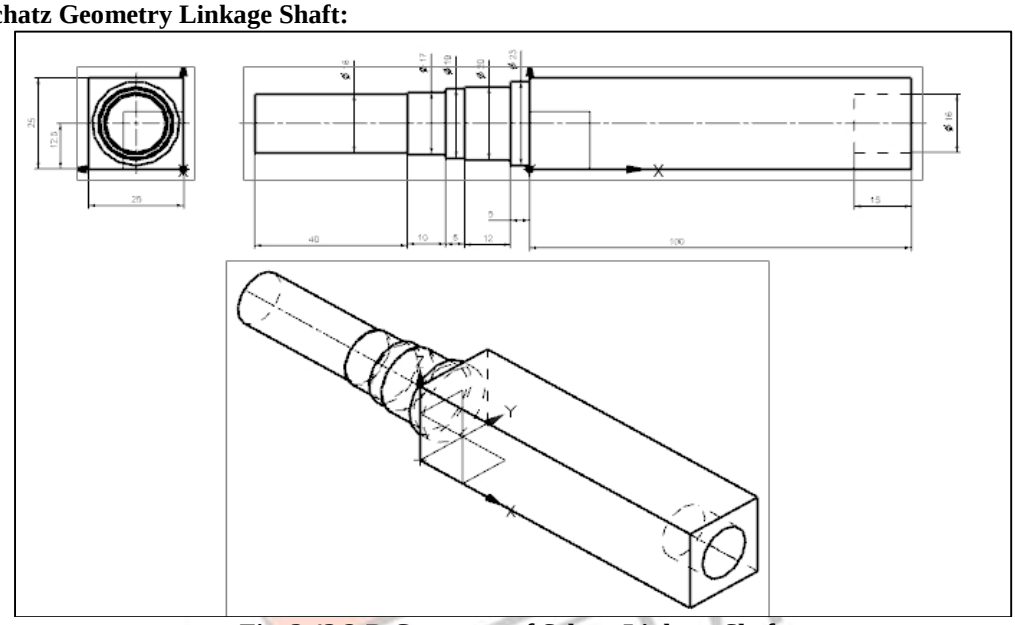

Fig. 3.43 2-D Geometry of Schatz Linkage Shaft

Table No. 3.17. Design data of Schatz Linkage Shaft

Designation	Ultimate Tensile Strength (N/mm^2)	Yield Strength (N/mm^2)
EN 24	800	680

Load = Torque / radius = 15120 /25 =604 N

$$fs_{allowable} = 0.18 \times 800 = 144\ N/mm^2$$

T design = 15.12 Nm

This is the allowable value of shear stress that can be induced in the shaft material for safe operation.

Check for torsional shear failure of shaft

$$Te = \frac{\pi \times fs_{act} \times d^3}{16}$$

$$fs_{act} = \frac{16 \times 15.12 \times 10^3}{\pi \times 16^3}$$

$$fs_{act} = 18.8\ N/mm^2$$

As; $fs_{act} < fs_{all}$

Schatz shaft is safe under torsional load.

M. Design of Hinge Pin

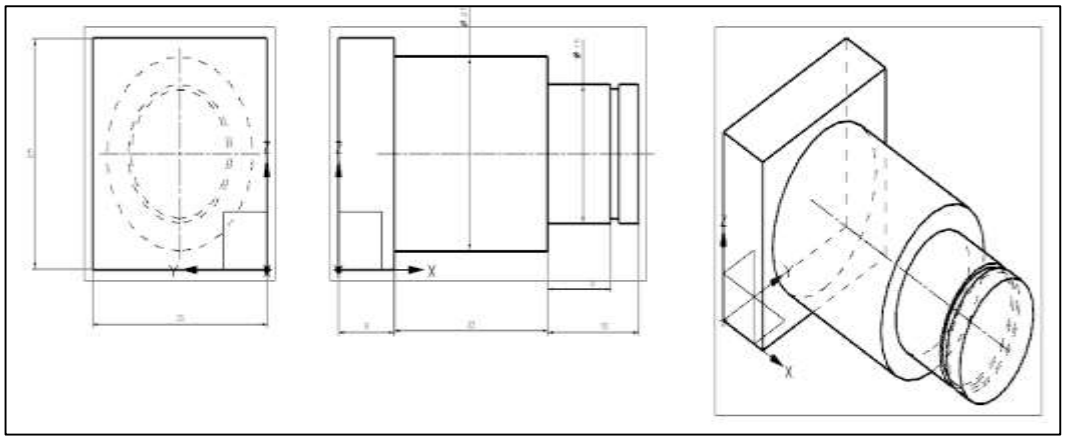

Fig. 3.49 Geometry of Hinge Pin

Table No. 3.19. Design data of Hinge Pin

Designation	**Tensile Strength N/mm²**	**Yield Strength N/mm²**
EN9	600	480

$$fsallowable = 0.18 \times 800 = 144\ N/mm^2$$

T design = 15.12 Nm

This is the allowable value of shear stress that can be induced in the shaft material for safe operation.

Check for torsional shear failure of hinge pin

$$Te = \frac{\pi \times fs_{act} \times d^3}{16}$$

$$fs_{act} = \frac{16 \times 15.12 \times 10^3}{\pi \times 16^3}$$

$$fs_{act} = 18.8\ N/mm^2$$

As; $fs_{act} < fs_{all}$

Hinge pin is safe under torsional load.

Direct Shear Stress Due to a Radial Load:-

Here radial load is due to the tangential load generated when the crank drives the connecting rod linkage at eccentricity of 25 mm

Load = Torque / radius = 15120 /25 =604 N

$$fs_{act} = \frac{W}{A}$$

$$fs_{act} = \frac{604 \times 4}{\pi \times 15^3}$$

$$fs_{act} = 3.41\ N/mm^2$$

As $fs_{act} < fs_{all}$

Hinge pin is safe under shear load.

N. Design of Schatz Bracket

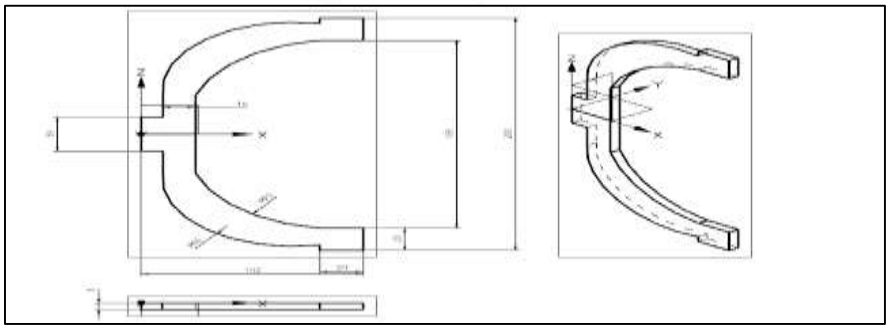

Fig. 3.55 2-D Geometry of Schatz Bracket

Direct Shear Stress Due to a Pull Load:

Load = Torque / radius = 15120 /25 =604 N

$$fs_{act} = \frac{W}{A}$$

$$fs_{act} = \frac{604}{6 \times 15}$$

$$fs_{act} = 6.71\ N/mm^2$$

As $fs_{act} < fs_{all}$

Schatz bracket is safe under shear load.

O. Design of Container Casing

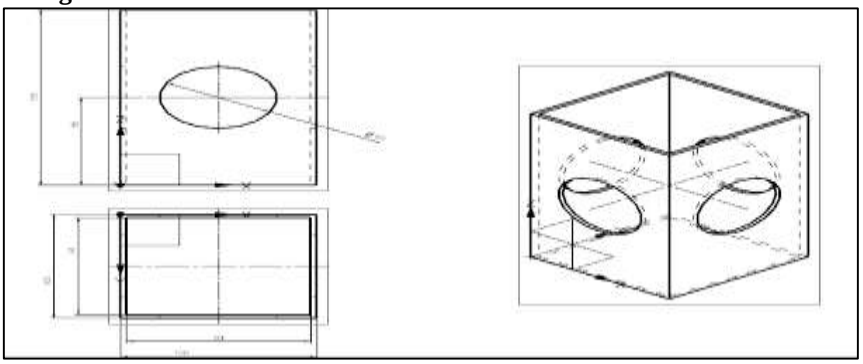

Fig. 3.61 2-D Geometry of Container Casing

Table No. 3.22. Design data of Container Casing

Designation	**Tensile Strength N/mm^2**	**Yield Strength N/mm^2**
Al	400	320

$$fs_{act} = \frac{W}{A}$$

$$fs_{act} = \frac{604}{(100 \times 100 - 94 \times 94 - 60 \times 60)}$$

$$fs_{act} = 0.75\ N/mm^2$$

As $fs_{act} < fs_{all}$

Casing is safe under shear load

7. RESULTS AND DISCUSSION

7.1 TEST AND COMPARISON OF TURBULA MIXER TO CONVENTIONAL MIXER

- **Conventional mixer:**

Fig. 4.1 Conventional Mixer

Mixer motor: 50 watt, 0 to 9500 rpm
Gear box: Worm gear box 1:60 ratio
Capacity: 3 litre
Test equipment used:

1. Viscometer
2. Glass and 0.6 mm wiper plate.

Observations: Conventional mixer

Table No. 4.1. Observations of Conventional mixer

Sr.No	Time min	Viscosity	Spreadability mm	Volume
01	3	4.6	130	-
02	6	4.4	132	-
03	9	4.4	136	-
04	12	4.2	140	-
05	15	4.1	146	2
06	20	4.1	148	3.1

Table No. 4.2. Observations of Turbula mixer

Sr.No	Time min	Viscosity	Spreadability mm	Volume
01	3	4.1	146	-
02	6	3.5	152	1
03	9	3.2	164	1.8
04	12	3.1	176	2.9
05	15	3.0	190	3.9
06	20	3.0	208	4.6

Comparative Graphs of Resultant Viscosity V/S Time

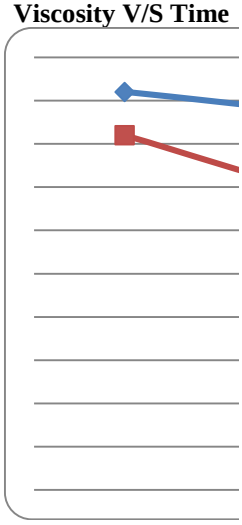

Fig. 4.2 Comparative Graphs of Resultant Viscosity V/S Time

Graph indicates the viscoisty of paint reduces with increase in time, lower paint viscosity is desirable characteristic. The Schatz geometry mixer shows better performance and better quality as compared to conventional mixer. Minimum paint viscoity obtained by the Schatz geometry mixer is close to 3 centipoise which is best desirable for maximum lustre and better application of paint along with least quanity of paint required per unit area of application.

Comparative Graph of Spreadablility of Paint V/S Time

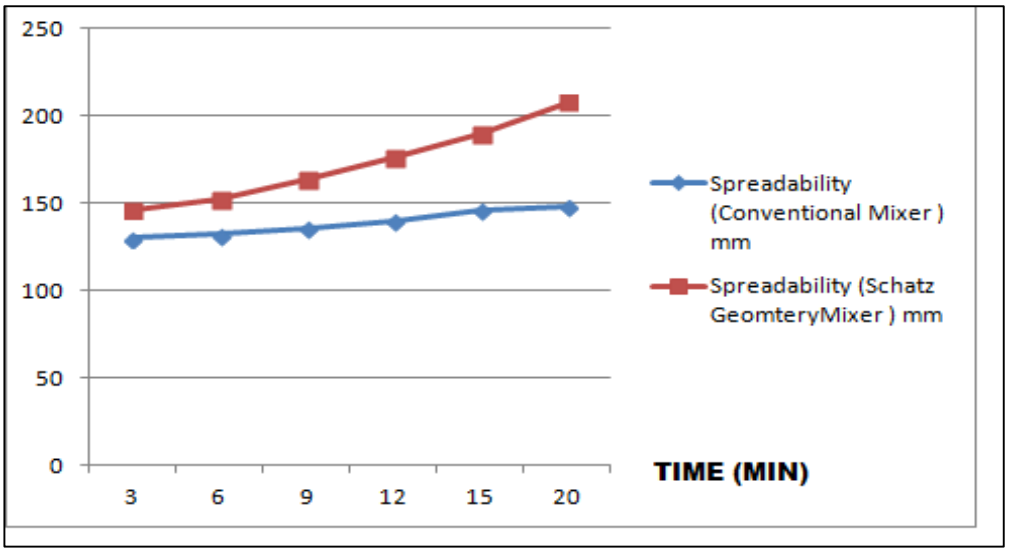

Fig. 4.3 Comparative Graph of Spreadablility of Paint V/S Time

The Schatz geometry mixer shows better performance and better spreadability as compared to conventional mixer. Maximum paint spreadability obtained by the Schatz geometry mixer is close to 200 mm which is best desirable for maximum lustre and better application of paint along with least quanity of paint required per unit area of application.

4.2 CONCLUSION

1. Productivity Effectiveness = $\frac{\text{Volume of Schatz geometry shaker mixer at 20 min}}{\text{Volume of Conventional Mixer at 20 min}}$

   Productivity Effectiveness = $\frac{4.61}{3.1}$ = 1.4837

   Thus the Schatz geometry mixer is 1.4837 times effective than the conventional mixer
2. Schatz mechanism with 3D-motion mixer gives the good quality homogeneous mixer. Intensive, fast and very gentle mixing of components of different density, size, shape and concentration.
3. Best mixing quality and no segregation due to the inversion kinematics.
4. High quality mixing results independent of vessel shape and without internal agitators.
5. Dust-free and hygienic mixing in closed containers.
6. Easy cleaning and maintenance.
7. Safety concept and mixing equipment as independent units.

REFERENCES

[1] Ingrid Bauman, Du Ska, Curi C and Matija Boban, "Mixing of Solids in Different Mixing Devices", Sadhana, Vol. 33, Part 6, December 2008, pp. 721–731.
[2] P.S.Jadhav, Prof. B.R.Jadhav, "A Study on Mixing of Composite Solids in the Three Dimensional Turbula Mixer", International Journal of Advanced Engineering Research and Studies, Vol. II, April-June, 2013, pp.138-141.
[3] P. S. Kulat, Prof. R. B. Chadge,"3d Motion Mixer for Material", International Journal of Pure and Applied Research in Engineering and Technology, Vol. 2 (9), 2014, pp.97-102.
[4] Douglas Bohl, Naratip Santitissadeekorn, Akshey Mehta, and Erik Bollt, "Characterization of Mixing in a Simple Paddle Mixer Using Experimentally Derived Velocity Fields", Clarkson University, pp.1-24.
[5] Yan Chen, "Design of Structural Mechanisms", Dissertation Submitted for the Degree of Doctor of Philosophy in Department of Engineering Science at the University of Oxford Trinity Term 2003.
[6] I. Bauman, "Solid-Solid Mixing with Static Mixers", Chem. Biochem. Eng, Vol. 15 (4), 2001, pp. 159–165.
[7] Dr. Bhawana Bhatt, "Pharmaceutical Engineering", Delhi Institute of Pharmaceutical science and research, pp 1-24.
[8] C-C Lee and J S Dai, "Configuration Analysis of the Schatz Linkage", Journal of Mechanical Engineering Science, Vol. 217, Part C, 2003, pp.779-786.
[9] Jiten Patel, G.K. Ananthasuresh, "A Kinematic Theory for Radially Foldable Planar Linkages", International Journal of Solids and Structures, Vol. 44, 2007, pp.6279–6298.